A Fully-integrated In-band OSNR Monitor using a Wavelength-tunable Silicon Microring Resonator and Photodiode

Qi Li[1*], Kishore Padmaraju[1], Dylan F. Logan[2,3], Jason J. Ackert[2], Andrew P. Knights[2], Keren Bergman[1]

1: Department of Electrical Engineering, Columbia University, 500 West 120th Street, New York, NY, USA
2: Department of Engineering Physics, McMaster University, 1280 Main Street West, Hamilton, ON, Canada
3: Currently with Ranovus Inc., Ottawa, ON, Canada
**ql2163@columbia.edu*

Abstract: We demonstrate a novel in-band OSNR monitor with full optical components integration. The OSNR monitor is shown to have a working range of 17 dB for 40-Gb/s OOK and DPSK signals, and is insensitive to chromatic dispersion of 0-250 ps/nm.

OCIS codes: (140.4780) Optical resonators; (060.4510) Optical communications; (230.3120) Integrated optics devices

1. Introduction

Driven by bandwidth-demanding applications and emerging broadband services, Internet backbone traffic continues to grow rapidly, increasing network complexity and presenting challenges in the management and control of optical networks. Optical performance monitoring (OPM) has been proposed for physical-layer fault management, maintenance, failure diagnosis as well as dynamic resource allocation capabilities [1]. As an essential part of OPM techniques, an optical signal-to-noise ratio (OSNR) monitor is an important tool to provide information on the signal transmission quality. With OSNR monitoring, impairment-aware optical networks can be realized using cross-layer communications, which can effectively counteract inter-channel impairments on the physical layer and meet the stringent quality-of-service (QoS) requirements of such networks [2].

Several OSNR monitoring methods have been proposed previously. One approach is the polarization-nulling method [3], which is based on the assumption that the signal is polarized while the noise is unpolarized. However, this technique may not be accurate when the noise is partially polarized or in the presence of polarization-mode dispersion (PMD), and it is difficult to realize in integrated optics. Another method, based on mach-zehnder interferometry [4-6], requires the prior knowledge of the signal amplitude autocorrelation function and therefore typically requires system calibration by turning off the noise and scanning signal interference [6]. Recently several efforts [7-9] have been made to realize OSNR monitoring in an integrated fashion, however these demonstrations still require discrete and bulky off-chip components such as power meters.

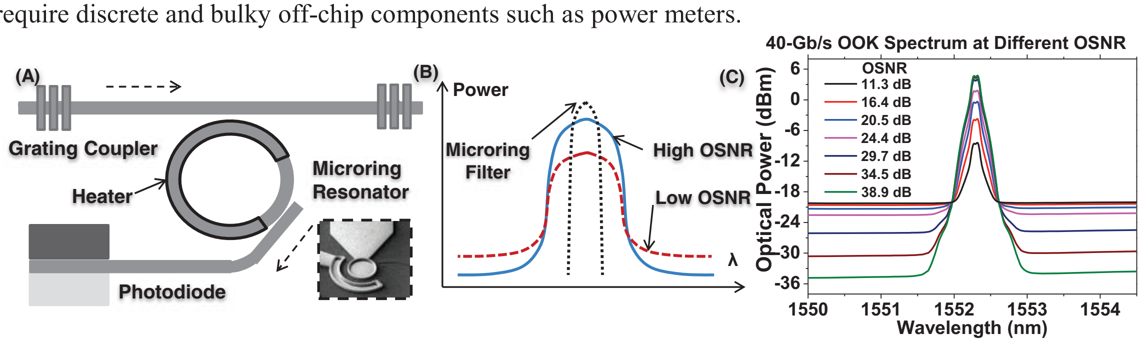

Fig. 1. (a) The OSNR monitor, composed of a microring resonator with integrated heater and silicon photodiode positioned on the drop port of the microring (not to scale). Inset: SEM image of fully processed device. (b) Working principle of the OSNR monitor. (c) Measured 40-Gb/s OOK spectrums at various OSNR.

In this work, we demonstrate an ultra-compact, modulation format and chromatic dispersion insensitive OSNR monitor, based on narrow-band filtering [10]. The high quality factor (Q) microring resonator acts as a band-pass filter to extract a portion of the signal spectrum with the in-band noise, which is detected by a defect-enhanced silicon photodiode [11] positioned at the drop port of the microring (Fig. 1a). Considering fixed optical power after amplifiers in an optical link, the channel power filtered by the microring increases with respect to higher OSNR (Fig. 1b). In the regime where the increment of filtered channel power is dominated by the signal power change, there is almost a linear relationship between the filtered channel power and the OSNR of that channel (Fig. 1b). This is also evident from equation (1):

$$OSNR\ (dB) = 10log_{10}\frac{P_{sig}}{P_{ASE}} = 10log_{10}\left(\frac{P_{total}}{P_{ASE}} - 1\right) \approx 10log_{10}\frac{P_{total}}{P_{ASE}} = P_{total} - P_{ASE}\ (both\ in\ dBm) \quad (1)$$

When changes in P_{total} are much larger than that of P_{ASE}, changes in OSNR increment can be approximated as changes in P_{total}. This is particularly true for low ONSR values, as shown for measured 40-Gb/s on-off keying (OOK) spectrums at various OSNR values (Fig. 1c).

2. Device and experiment

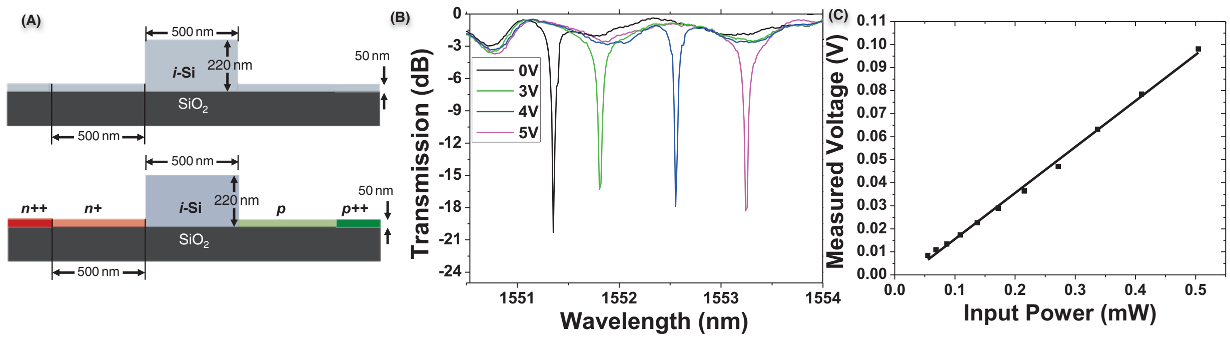

Fig. 2. (a) Waveguide geometry and doping profile for the microring (top) and silicon photodiode (bottem). (b) Transmission spectra of the microring at different heater voltages. (b) Measurement of the silicon photodiode linearity.

The 15-μm radius microring used in this experiment, with a Q of ~17000, is used as a band-pass filter with ~ 0.09nm (11 GHz) 3dB passband. Situated 1 μm above the microring, a thin film titanium-based heater is used to tune the resonance of the microring (Fig. 2b). The wavelength tunability of the microring resonator using the integrated heater makes it applicable to dense wavelength division multiplexing (WDM) environments, since the thermal tuning can be used to monitor different channels and to stabilize the microring resonance with respect to temperature and optical power [14] at the same time. A defect-enhanced silicon photodiode is integrated at the drop port of the microring to measure the filtered optical power. The generated photocurrent is converted to the measured voltage using a transimpedance amplifier (TIA). The linearity of the photodiode response is tested at the 1551.3 nm resonance (Fig. 2c). The silicon microring and photodiode based ONSR monitor is fully integrated on a chip area of ~ 0.15 mm^2. A polarization controller is used to ensure TE polarized light is coupled into the chip with holographic grating couplers. In future implementations, the polarization controller can be eliminated by using an on-chip polarization-independent scheme [15]. Silicon microring resonators have been proposed in many applications including on-chip interconnects, optical access networks, as well as large scale computing systems [12-13]. Since both the silicon microring resonator and the defect-enhanced silicon photodiode are CMOS-compatible, they can leverage mature CMOS fabrication technology to be produced at the economy-of-scale required for mass deployment in OPM networks. Furthermore, the ultra-compact OSNR monitor, once integrated with microelectronics, will enable direct measurement of OSNR under stringent footprint, power and cost requirements.

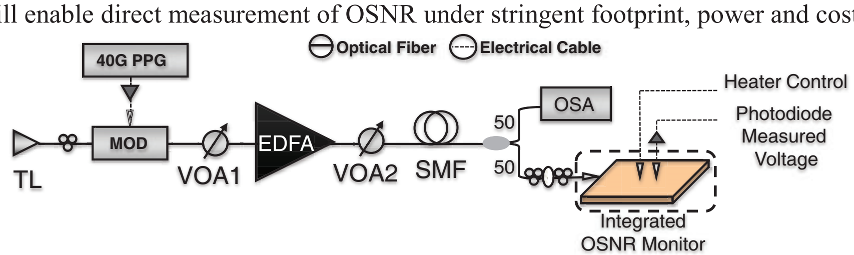

Fig. 3. Experimental Setup.

In our experiment (Fig. 3), a tunable laser (TL) is modulated by a phase modulator (MOD) at 40-Gb/s, driven by a 2^{15}-1 pseudo-random bit sequence (PRBS) signal from a pulse pattern generator (PPG). The generated signal is then degraded by a variable optical attenuator (VOA1) and then amplified by an erbium-doped fiber amplifier (EDFA) to introduce a controlled amount of ASE noise and thus vary its OSNR. The signal then goes through different lengths of single-mode fiber (SMF) to introduce different amounts of chromatic dispersion. The second attenuator (VOA2) is used to ensure that the same optical power (1 dBm) reaches the chip in all trials. A portion of the signal is sent to an optical spectrum analyzer (OSA) for OSNR verification, and the other portion is coupled into the silicon chip by a grating coupler. The heater voltage is optimized to achieve maximal photodiode voltage for both modulation formats. The photodiode voltage is recorded for OSNR measurement.

Figure 4a shows measurement results for the 40-Gb/s OOK and differential phase-shift keying (DPSK) channels at varying OSNR values. The recorded photodiode voltages are normalized against the maximum values for both cases. For both modulation formats, the linear range of the measured voltages is around 17 dB (17dB to 32 dB for OOK, 10 dB to 27 dB for DPSK). Note that the measured voltage is dependent on the TIA gain, therefore, the dynamic range of the voltage can be tailored as necessary for the specific application. When the OSNR is above the upper bound, the measure voltage tends to saturate because there is a smaller difference in terms of filtered power in high OSNR regions [10]. The sensitivity of the OSNR monitor is expected to be improved when using microring resonators with higher Q [8].

The 40-Gb/s signals are also propagated through 0-, 5-, 10-, and 15- km lengths of SMF to validate the insensitivity to chromatic dispersion of the demonstrated OSNR monitor (Fig. 4b). The measured voltage has a small variation (< 10%) for all the signals with different OSNR. The voltage difference is partially due to fluctuations in the optical power at the input of the chip. The PMD sensitivity of the OSNR monitor was not tested; however a demonstrated scheme based on the same principle has been shown to be insensitive to PMD of 0-50 ps [10].

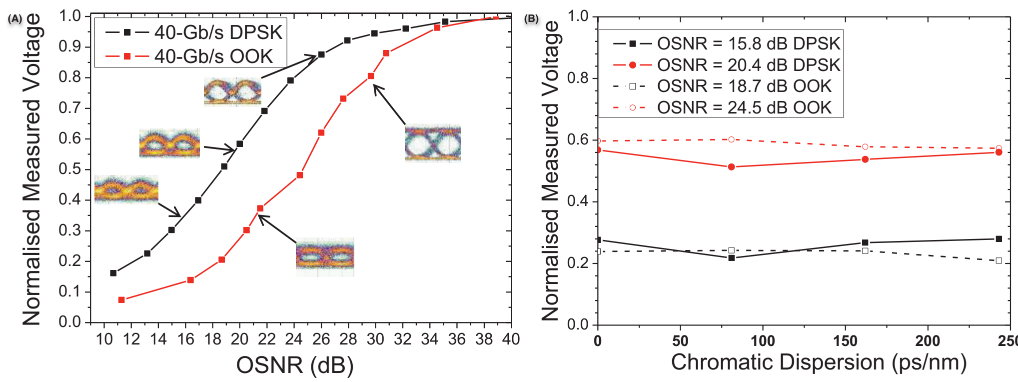

Fig. 4. (a) Normalized measured photodiode voltage as a function of OSNR. Insets: eye diagram of the 40-Gb/s OOK and demodulated DPSK signals. (b) Normalized measured photodiode voltage as a function of chromatic dispersion with different OSNR.

3. Conclusion

We have demonstrated a simple and ultra-compact in-band OSNR monitor using an integrated wavelength-tunable silicon microring resonator and photodiode. The OSNR monitor has a working range of 17 dB, and was measured to be insensitive to chromatic dispersion levels of 0-250 ps/nm. The scheme can also be easily extended to monitor signals with other modulation formats and data rates. Based on silicon photonic components, the demonstrated OSNR monitor has the potential to be low cost and be directly integrated with auxiliary microelectronics. In addition, with the maturing of silicon photonics technology [16], OSNR monitors based on other principles such as the 1-bit [4] or ¼-bit [5] delay line interferometers, can also be fabricated in one single chip, enabling powerful OPM components for future impairment-aware optical networks.

This work was supported in part by the NSF through CIAN ERC under Grant EEC-0812072. This work was also supported by the Natural Sciences and Engineering Research Council of Canada. Additionally, we are grateful to CMC Microsystems and IME Singapore for enabling work in the design and fabrication of the silicon photonic chips.

4. References

[1] D. C. Kilper et al. "Optical performance monitoring." IEEE/OSA J. Lightw. Technol. 22.1 (2004): 294-304.
[2] F. Fidler et al. "Impairment-aware optical networking using cross-layer communication." IEEE J. Opt. Commun. Netw. 5.2 (2013): 144-158.
[3] J. H. Lee et al. "OSNR monitoring technique using polarization-nulling method." IEEE Photon. Technol. Lett. 13.1 (2001): 88-90.
[4] X. Liu et al. "OSNR monitoring method for OOK and DPSK based on optical delay interferometer." IEEE Photon. Technol. Lett. 19(15): 1172-1174 (2007).
[5] Y. K. Lizé et al. "Simultaneous and independent monitoring of OSNR, chromatic and polarization mode dispersion for NRZ-OOK, DPSK and duobinary." OFC, 2007.
[6] E. Floodet al. "In-band OSNR monitoring using a pair of Michelson fiber interferometers." Opt. Express 18.4 (2010): 3618-3625.
[7] L. Jia et al. "Integrated in-band optical signal-to-noise ratio monitor implemented on SOI platform." Opt. Express 20.8 (2012): 8512-8517.
[8] K. Xu et al. "An Ultracompact OSNR Monitor Based on an Integrated Silicon Microdisk Resonator." IEEE Photon. J. (2012): 1365-1371.
[9] F. Morichetti et al. "High-Sensitivity In-Band OSNR Monitoring System Integrated on a Silicon Photonics Chip," IEEE Photon. Technol. Lett. 25(19), 1939-1942 (2013).
[10] J-Y. Yang et al. "Optical signal-to-noise ratio monitoring of an 80 Gbits/s polarization-multiplexed return-to-zero differential phase-shift keying channel." Optics Letters 34.7 (2009): 1006-1008.
[11] D. F. Logan et al. "Monitoring and tuning micro-ring properties using defect-enhanced silicon photodiodes at 1550 nm." IEEE Photon. Technol. Lett. 24.4 (2012): 261-263.
[12] D. Thomson et al. "50-Gb/s silicon optical modulator." IEEE Photon. Technol. Lett. 24.4 (2012): 234-236..
[13] G. Dongaonkar et al. "Ultra-low Latency Optical Switching for Short Message Sizes in Cluster Scale Systems," IEEE Optical Interconnects 2013 TuB2.
[14] Q. Li et al. "Experimental characterization of the optical-power upper bound in a silicon microring modulator." IEEE Optical Interconnects 2012 TuB5.
[15] C. Li et al. "Monolithic Integrated Silicon Polarization-Independent Tunable Filter Circuit With Germanium pin Photodetector." IEEE Photon. Technol. Lett. 24.9 (2012): 781-783.
[16] C. Galland et al. "Systems and Devices in a 30 GHz Silicon-on-insulator Platform," ECOC 2013 Mo.3.B.2.